Overview of Novel Post-Processing Techniques to Reduce Uncertainty in Antenna Measurements

Manuel Sierra-Castañer, Alfonso Muñoz-Acevedo,
Francisco Cano-Fácila and Sara Burgos
*Technical University of Madrid (Universidad Politécnica de Madrid - UPM),
Spain*

1. Introduction

The error analysis has been investigated since 1975 since recent publications, as shown in references as (Newell et al., 1975) where the classical 18 terms for planar near field systems where established. It is also worth mentioning the more recent studies developed inside the actions under the "Antenna Measurement" activity of the "Antenna Centre of Excellence (ACE)" within the sixth framework research program of the European Union. In particular, that work pretended to establish common error calculation criteria in spherical near-field and far-field antenna measurement systems. The results of that research were summarized in an exhaustive deliverable (Alexandridis et al., 2007), which detailed the observations stated by several research institutions. In that deliverable it was agreed that the causes of uncertainties and errors in a spherical near-field antenna measurement are divided in six categories:

1. **Mechanical uncertainties and errors**: this group includes the axes intersection, the axes orthogonality, the horizontal pointing, the probe vertical position, the probe horizontal and vertical pointing and the measurement distances.
2. **Electrical uncertainties and errors**: this class contains the amplitude and phase drift, the amplitude and phase noise, the leakage and crosstalk, the amplitude non-linearity and the amplitude and phase shift in rotary joints.
3. **Probe-related uncertainties and errors**: this kind of uncertainties takes into account the channel balance amplitude and phase, the polarization amplitude and phase and the pattern knowledge.
4. **Stray signals**: this type of uncertainties consists of the multiple reflections, the room scattering and the AUT support scattering.
5. **Acquisitions errors**: this group involves the scan area truncation and the sampling point offset.
6. **Processing uncertainties and errors**: in this group the spherical mode truncation and the total radiated power are considered.

The second part of the chapter will deal with the description of four different classes of correction techniques for antenna measurements.:

1. Averaging and comparison of measured antenna radiation patterns: pattern comparison technique is a very useful technique to evaluate the quality of the quiet zone in far field systems. This technique can also be used for cancelling source of errors, averaging two measurements including opposite errors. The easiest way is the averaging of two measurements where the distance between the AUT and antenna probe has been modified in a quarter of wavelength: in this case the difference of the reflected rays in both configurations is $\lambda/2$ (180 deg), so the averaging of both acquisitions cancels the effect of this reflection.

2. Application of source reconstruction techniques to reduce the effect of the noise, leakage and scattering: a source reconstruction technique is a method used to obtain the field or the equivalent currents distribution over the antenna under test (AUT) plane from the knowledge of its radiated field (near- or far-field). This information can be employed to identify errors, e.g., electrical errors in arrays or mechanical errors in reflectors. Apart from its classic application, a diagnostic process also gives a complete electromagnetic characterization of the antenna, which is the basis of other applications, like near- to far-field transformations. In this work, the additional information provided by a diagnostic technique is employed to reduce the effect of three common errors in antenna measurements: reflections, noise and leakage.

3. Iterative algorithms to reduce the truncation error in planar, cylindrical and not complete spherical acquisitions: other alternatives to reduce errors in antenna measurements are based on iterative algorithms. This is the case, the method proposed to reduce truncation errors when the measurement is performed over a surface that does not fully enclose the AUT (plane, cylinder or partial sphere). The method is based on the Gerchberg-Papoulis iterative algorithm (Gerchberg, 1974) and (Papoulis, 1975) used to extrapolate band-limited functions and it is able to extend the valid region of the calculated far-field pattern up to the whole forward hemisphere. The extension of the valid region is achieved by applying iteratively a transformation between two different domains.

4. Techniques to improve the quality of the quiet zone in compact ranges: CATR measurement facilities are characterised by a straightforward operation which is able to perform real time antenna measurements along a wide margin of frequencies, whenever reflectors or lenses are used as collimators. In spite of their compactness, CATR facilities operate in far-field conditions, which mean that the test wave received by the AUT should be a plane wave. The operation of a CATR relies on the planarity of this test wave, inside the "quiet zone" volume.

This paper is divided as follows: section 2 explains the main uncertainty sources based on the works developed on the Antenna Centre of Excellence (Alexandridis, 2007). Sections 3 to 6 detail the different aspects mentioned before, including some practical examples.

2. Revision of the uncertainty sources involved in the directivity and gain determinations

The uncertainty constitutes the measure of the quality of a measurement, which allows comparing the measurement results with other outcomes, references, specifications or standards. In order to determine how the uncertainties may influence the measurement results, it is worth reviewing the methodology that allows evaluating the uncertainties in the measured outcomes. (Taylor et al. 1994), (ISO/IEC 98, 1995) and (Gentle et al., 2003) are good basic representative guides, where the general methods to estimate the uncertainty are

widely explained. Actually, the above mentioned studies of Hansen in (Hansen, 1988) and Newell in (Newell, 1988), published in 1988 and concerning the uncertainties in antenna measurements, settle the basis to evaluate the inaccuracies that may affect the results achieved from the antenna measurements. However, as the technology has incredibly evolved since then, an update of the uncertainty analysis is considered appropriate and therefore, this section will try to cover the uncertainty study of measurements that nowadays could be carried in indoor facilities, summarizing the work developed in (Alexandridis et al., 2007), under the "Antenna Measurement" activity of the "Antenna Centre of Excellence (ACE)" within the sixth framework research program of the European Union, involving researchers from the National Center of Scientic Research "Demokritos" (NCSRD), the Technical University of Denmark (DTU), the Technical University of Madrid (UPM), SATIMO (Société d'Applications Technologiques de l'Imagerie Micro-Onde S.A.), Saabgroup, FTR&D (France Telecom Recherche & Développement) and IMST GmbH. In particular, that work pretended to establish common error calculation criteria in spherical near-field and far-field antenna measurement systems. Thus, the outcomes of this activity became important instruments to verify the measurement accuracies for each range and to investigate and evaluate possible improvements in measurement set-up and procedures.

It was seen in this research that these errors depend not only on the gain determination technique applied to establish the antenna gain, but also on the AUT that will be measured and on the measurement range employed. Hence, a generic evaluation cannot be carried out and in each case the study has to be particularized and adapted to the AUT and measurement facility considered.

Besides, it is noticeable that the procedure to evaluate the uncertainties has to be different in the near-field systems than in the far-field ranges. This is due to the fact that in the far-field systems the measurement is direct and thus, the uncertainty could also straightly be obtained. On the other hand, in near-field ranges the information and the uncertainties related to this data are processed and so the near-to-far-field transformation has an influence on the both magnitudes. The sources of uncertainty present in the near-field measurements are either systematic or random quantities. The systematic errors can be characterized using the mean. On the other hand, for the random sources of uncertainties, the mean, the variance (σ^2) and the probability distribution are employed to carry out the description of the magnitude studied. The first step to accomplish a complete uncertainty study is to identify all the sources of inaccuracies (uncertainties or errors) affecting the measurements. In the exhaustive deliverable carried out under the "Antenna Measurement" activity of the ACE, the observations, stated by the participant research institutions, were detailed and the causes of uncertainties and errors in a spherical near-field antenna measurement were divided in six categories:

1. Mechanical uncertainties and errors: this group includes the axes intersection, the axes orthogonality, the horizontal pointing, the probe vertical position, the probe pointing and the measurement distances. Fig. 1 illustrates how is defined a non-intersection error in a spherical coordinate system.
2. Electrical uncertainties and errors: this class contains the amplitude and phase drift, the amplitude and phase noise, the leakage and crosstalk, the amplitude non-linearity and the amplitude and phase shift in rotary joints.
3. Probe-related uncertainties and errors: this kind of uncertainties takes into account the channel balance amplitude and phase, the polarization amplitude and phase and the

pattern knowledge. In Fig. 1 "P1" and "P2" are the lineal polarization relations in each port and "Q1" and "Q2" the circular polarization relations in each port.

4. Stray signals: this type of uncertainties consists of the multiple reflections, the room scattering and the AUT support scattering. Fig. 3 shows a schematic representation of these types of reflections in an anechoic chamber.

5. Acquisitions errors: this group involves the scan area truncation and the sampling point offset.

6. Processing uncertainties and errors: in this group the spherical mode truncation and the total radiated power are considered.
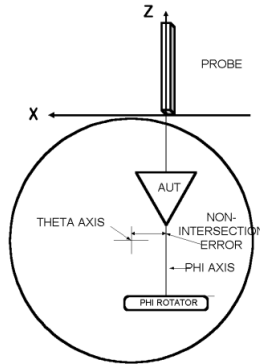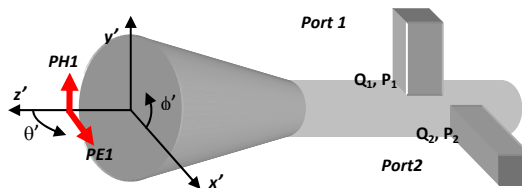

Fig. 1. Non-intersection error.
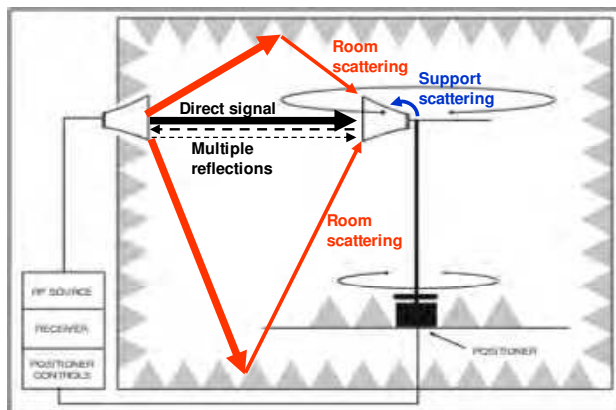

Fig. 2. Ports of a dual-polarized probe.

Fig. 3. Different reflections and scattering in an anechoic chamber.

Table 1 summarizes all the uncertainties and errors related to peak directivity in spherical near-field measurement that contribute to the total uncertainty, assuming that the probe is not an array. This table has extended the results from spherical near-field systems to a more general acquisition. Some of the terms affect more spherical systems and other ones are more important for cylindrical or planar systems.

Category	Uncertainty	Description
Mechanical	1. Axes intersection	Lateral displacement between the horizontal and vertical axes
	2. Axes orthogonality	Difference from 90° of the angle between the horizontal and vertical axes
	3. Horizontal pointing	For $\theta = 0°$, horizontal mispointing of the horizontal axis to the probe reference point
	4. Probe vertical position	Vertical displacement of the probe reference point from the horizontal axis
	5. Probe horizontal and vertical pointing	Horizontal or vertical mispointing of the probe z-axis
	6. Measurement distance	Error in the measurement of the distance between the AUT and probe reference point
Electrical	7. Amplitude and phase drift	Systematic amplitude and phase change at still AUT
	8. Amplitude and phase noise	Random amplitude and phase change at still AUT
	9. Leakage and crosstalk	Extraneous signal dependent on angle
	10. Amplitude non-linearity	Difference from linear dependence of measured value versus input signal level
	11. Amplitude and phase shift in rotary joints	Systematic amplitude and phase change with angle of rotary joints
Probe-related	12. Channel balance amplitude and phase	Amplitude and phase difference between the two polarization channels
	13. Polarization amplitude and phase	Amplitude and phase of the probe polarization coefficients
	14. Pattern knowledge	Deviation of the known or assumed probe pattern from the true one
Stray signals	15. Multiple reflections	Contribution to the received signal due to interactions between the AUT and the probe
	16. Room scattering	Contribution to the received signal due to finite reflectivity of the anechoic chamber
	17. AUT support scattering	Contribution to the received signal due to scattering from the AUT support structure
Acquisition	18. Scan area truncation	Error due to partial sphere, cylinder or plane acquisition
	19. Sampling point offset	Error due to continuous positioner rotation
Processing	20. Spherical mode truncation	Changes in the far-field due to different number of modes included in the field calculation
	21. Total radiated power	Error in the calculation of the total power

Table 1. Summary of uncertainty contributions.

3. Averaging and comparison of measured antenna radiation patterns

The comparison among patterns, or pattern comparison technique, is a very well known technique to evaluate the performance on an antenna measurement system. For instance, Fig. 4 shows the patterns measured in far field for the same antenna, but sliding the probe to different positions. The change in the distance between AUT and antenna probe makes completely different the interference between the direct ray, the reflected rays in the walls of the anechoic chamber and the multiple reflections between AUT and antenna probe positioners and absorbers. As it is observed in Fig. 4, the effect is negligible in the co-polar peak, since the level of the direct ray is much higher than the level of the reflected ray. However, the effect is noticeable for the cross-polar radiation and the side lobes. Assuming that the main effect is due to multiple reflections between AUT and antenna probe, if the distance between probe and AUT is moved a quarter of the wavelength, the total distance of the ray due to the first reflection is a half of the wavelength larger. A vectorial addition of both contributions eliminates the effect of this first reflection, while the two direct rays are added in quadrature. Also, if the distance is modified half wavelength, the direct rays are with opposite phase while the first reflections are with the same phase. Therefore, a vectorial subtraction of both magnitudes also cancels the reflected rays.
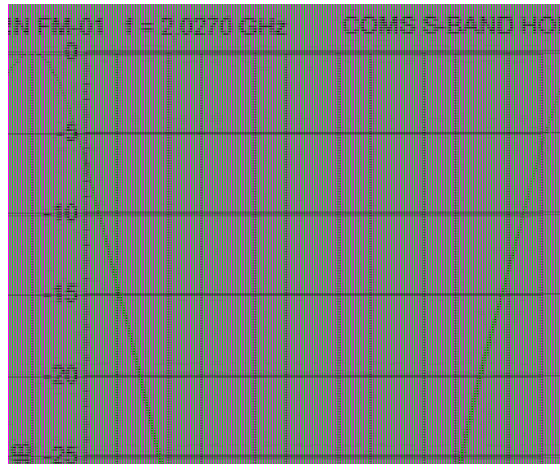

Fig. 4. Measurement of a horn antenna at different probe to AUT distances.

This technique has been applied to the measurements of the VAST12 ("12 GHz Validation Standard Antenna") designed and manufactured at the Technical University of Denmark in 1992 under the contract from the European Space Research and Technology Center and used as Reference antenna for intercomparison purposes. Fig. 6 shows the application of this technique for the measurement of the VAST12 antenna. There, both individual patterns are compared with the averaged pattern, and a slightly improvement in the crosspolar is observed. For the side lobe levels, it is not possible any improvement, since they can be affected by reflections in the walls (not corrected with this averaging). This technique can also be applied to reduce the effect of the scattering in the walls. However, in this case, the sliding has to be different, since half wavelength should be the difference between the direct ray and the reflected ray in the walls. Since the scatterers can be at different positions, a compensation technique is the measurement at different distances and the vectorial

averaging of them. In this case, the averaging does not cancel the effect of the scattering, but reduces its effect. Also, in (Burgos, 2009), this technique was used to reduce the effect of the mechanical uncertainties due to the positioners and the gravity effect. Four different full-sphere acquisitions schemes were developed, as it is shown in Fig. 7. The far field was averaged and the results are compared with the individual patterns (Fig. 8). In this case, there is one individual acquisition scheme that clearly shows some problems (mainly due to reflections in the chamber). The averaged far field corrects clearly this problem, as it is observed in the crosspolar and in the side lobe levels.
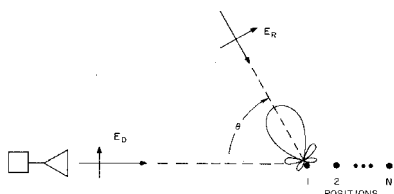

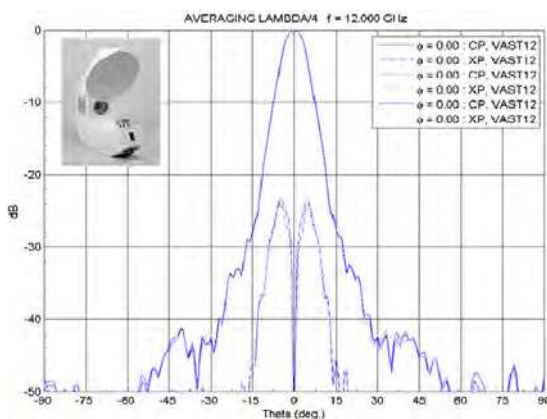Fig. 5. Sliding for the room scattering compensation.

Fig. 6. Measurement of VAST12 antenna at two AUT distances and averaging.
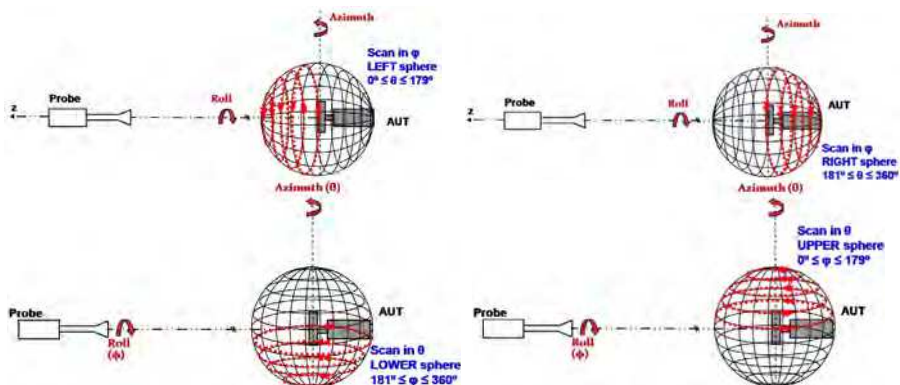

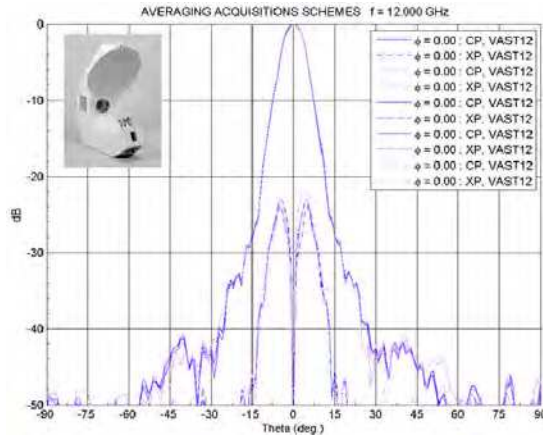Fig. 7. Four different full sphere acquisitions schemes.

Fig. 8. Measurement of VAST12 antenna for the four acquisition schemes and averaging.

4. Application of source reconstruction techniques to reduce the effect of the noise, leakage and scattering

A sources reconstruction technique is a method to obtain the extreme near-field or the equivalent currents distribution of an antenna from the knowledge of its radiated field (near or far field). This information can be employed to detect errors, and also identify which are the causes of such errors, for example, electrical errors in arrays or mechanical errors in reflectors. Apart from its classic application, a diagnostic process also gives a complete electromagnetic characterization of the antenna, which is the basis of other applications, like near- to far-field transformations, radome applications, radioelectric coverage, etc. In this work, that additional information is employed to reduce the effect of common errors in antenna measurements.

Basically, diagnostic techniques can be divided into two types. The first of them is based on the equivalence principle and the integral equations relating fields and sources (integral equation methods), and the second one on modal expansions (modal expansion methods). Integral equation methods have general characteristics, but from a numerical point of view they are more complex than modal expansion methods because it is necessary to solve a system of integral equations. Several approaches to obtain a solution of such a system (sources from the radiated field) have been studied in (Alvarez, 2007) and (Petre, 1992) for different measurement setup geometries. In these studies, a system of integral equations (1) is solved by using a numerical method like the Finite Difference Time Domain (FDTD) method, the Finite Element Method (FEM), or the Method of Moments (MoM).

$$\vec{E}_{meas}\left(\vec{r}\right) = -\iint_{S_0} \overline{M}\left(\vec{r}'\right) \times \nabla G\left(\vec{r},\vec{r}'\right)ds' \tag{1}$$

where $\vec{E}_{meas}\left(\vec{r}\right)$ is the measured electric field at the observation point $\vec{r}$, $\vec{M}\left(\vec{r}\right)$ represents the equivalent magnetic current at the source point within the reconstruction surface S_o, and $G\left(\vec{r},\vec{r}'\right)$ symbolizes the three-dimensional Green function.

On the other side, modal expansion methods require lower computational complexity, but due to the fact that the measured field has to be expressed as a superposition of orthogonal functions (vector wave solutions), they can only be used in particular situations, i.e., when the measurement is performed over canonical surfaces; planar, cylindrical and spherical are normally used because complex mechanical scannings are not required. Depending on the coordinate system, one particular kind of expansion (plane wave expansion, cylindrical wave expansion or spherical wave expansion) is carried out (Yaghjian, 1986) and (Johnson, 1973). Then, the plane wave spectrum (PWS) is calculated from the corresponding expansion, and the field over the antenna aperture can be directly obtained once the PWS is known, as shown in (2).

$$\vec{E}_{ap}\left(x,y\right)=\frac{1}{2\pi}\int_{-\infty}^{\infty}\int_{-\infty}^{\infty}\vec{P}\left(k_x,k_y\right)\cdot e^{-j\left(k_x x+k_y y\right)}dk_x dk_y \tag{2}$$

where $P(k_x,k_y)$ stands for the electric field PWS in the (k_x,k_y) direction. The last step is to explain how to obtain the PWS from the modal expansions. In planar near-field measurements, the PWS is directly obtained from the modal expansion of the samples. However, this PWS is referenced to the measurement plane, and a back-propagation to the AUT plane (Wang, 1988) has to be used to determine the appropriate PWS. For the spherical near-field case, a transformation from a spherical wave expansion to a plane wave expansion (SWE-to-PWE) is required. This transformation was recently developed in (Cappellin, 2008) and relates spherical and plane coefficients. If a measurement is to be performed in a cylindrical near-field system, up to now there have been no publications explaining the approach to calculate the PWS from the cylindrical coefficients. In this case, the only solution is to apply a cylindrical near-field to far-field transformation (Yaghjian, 1986) and (Johnson, 1973). Next, the PWS components are obtained by solving the system of equations specified in (3).

$$\begin{cases} E_\theta\left(r,\theta,\phi\right)=j\dfrac{ke^{-jkr}}{r}\left\{\cos\phi\cdot P_x(k_x,k_y)+sin\phi\cdot P_y(k_x,k_y)\right\} \\[2mm] E_\phi\left(r,\theta,\phi\right)=j\dfrac{ke^{-jkr}}{r}\cos\theta\left\{\cos\phi\cdot P_y(k_x,k_y)-sin\phi\cdot P_x(k_x,k_y)\right\} \end{cases} \tag{3}$$

This information provided can be used as the basis of methods to suppress certain errors when measuring an antenna. In this work, the next three methods are proposed.

4.1 Reflection suppression method

Normally, the antenna measurements are carried out in anechoic chambers to reduce unwanted contributions, such as reflections or diffractions from the environment. However, there are special cases in which the use of that kind of measurement setup is not possible, and a semi-anechoic chamber or an outdoor measurement system has to be employed. In fact, reflection waves may also appear in anechoic chambers due to imperfections in the radiation absorbing material (RAM). In any case, when the measurement is not performed in a fully anechoic environment, the unwanted contributions could significantly alter the actual antenna properties, producing a ripple in the radiation pattern.

The number of approaches to analyze and cancel the effects of unwanted contributions has increased in recent years. There are methods that are employed not to remove the reflection

waves, but rather to characterize the chambers by a figure of merit, usually called the reflectivity level, in frequency domain (Appel-Hansen, 1973) or time domain (Clouston, 1988). Another method, based on measurements at several distances, was presented (Nagatoshi, 2008). Other solutions within the category of so-called compensation methods can be applied to avoid measuring the AUT several times at different distances with respect to the probe (Black, 1995) and (Leatherwood, 2001). Time-gating techniques can also be employed as an option to remove reflected contributions, as it has been presented in (Young, 1973) and (Burrell, 1973). However, the complexity of the pieces of equipment is lower when using frequency-domain measurements as proposed in (Loredo, 2004).

The proposed method is based on a diagnostic technique. The input data are taken over only one arbitrary surface in the frequency-domain. Moreover, compared with some time-gating techniques or frequency decomposition techniques, it is not necessary to measure more than one frequency. Therefore, the measurement time is reduced considerably and, because the frequency-domain is employed, complicated equipment is not needed. If reflected waves are present in antenna measurements, the radiation properties obtained will be perturbed. These same incorrect results are achieved with an equivalent system where reflections can be viewed as direct waves coming from virtual sources, as shown in Fig. 9 (a). Such a replacement is explained in detail via image theory, which was also used in (Lytle, 1972) to study ground reflections as image current distributions. The identification of the virtual sources is not possible with a conventional diagnostic technique, where the field is only reconstructed over the antenna aperture. However, if the field reconstruction is performed over a surface larger than the antenna dimensions, the aforementioned fictitious sources can be found and cancelled with a filtering process.

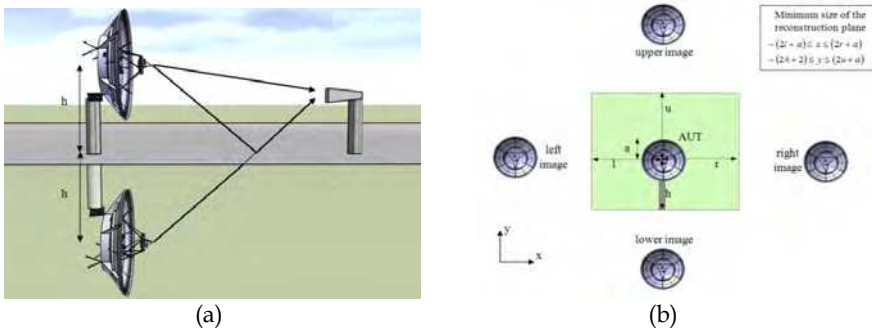| (a) | (b) |

Fig. 9. (a) Reflections in antenna measurements viewed by means of image theory; (b) Image theory in a general case with reflections on the floor, the ceiling and the side walls.

By applying any of the reconstruction methods explained before, the extended reconstructed field can be found. In the reconstructed domain, real sources and virtual sources are not spatially coincident. Therefore, a spatial filtering can be applied to suppress those virtual sources associated to the reflections. This filtering is defined as follows

$$F_1(x,y) = \begin{cases} 1 & \forall\ (x,y) \notin Z_V \\ 0 & \forall\ (x,y) \in Z_V \end{cases} \tag{4}$$

where Z_V represents the zone where virtual sources are placed.

The steps of the algorithm that implements the proposed method are depicted in detail in Fig. 10. This method is a generic approach because it can be used with any kind of measurement. The only thing to keep in mind is the proper selection of the diagnostic technique. Regardless of the method choice, after the diagnostic stage, the field distribution over the extended AUT plane is known, and virtual sources can be identified. Then, these sources are filtered out by employing the spatial filtering defined in (4). Finally, a new corrected PWS is obtained by taking the inverse Fourier transform of this filtered field distribution.
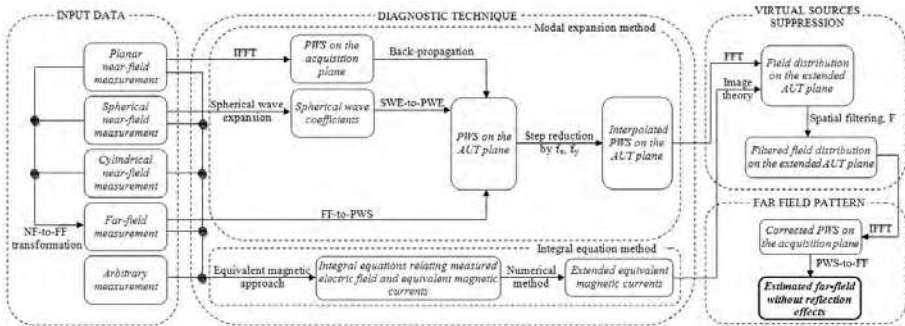

Fig. 10. Diagram of the reflection suppression method.

To verify the accuracy of the presented method, a measurement using the planar near-field range in the antenna test facility of the Technical University of Madrid (UPM) was performed. For the experiment, the probe and the AUT were selected to be a corrugated conical-horn antenna and a pyramidal-horn antenna, respectively, and they were separated from each other by 1.57 m. A reference measurement over a 2.4 m × 2.4 m acquisition plane was recorded in order to have a pattern with which to compare the future results with reflections and reflection suppression. Then, a rectangular metallic plate was placed in the
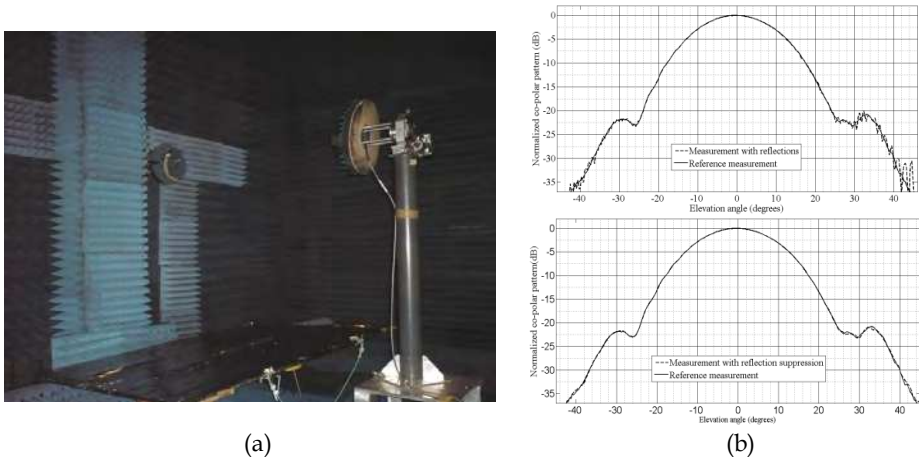

(a)   (b)

Fig. 11. (a) Experimental setup with a metallic plate; (b) Comparison between the reference pattern and the pattern with reflections for the φ=90°; (c) Comparison between the reference pattern and the pattern with reflection suppression for the φ=90°.

anechoic chamber, as see in Fig. 11(a), so as to introduce reflections in the measurement with the AUT at a height of 1.3 m above the plate. Fig. 11(b) shows a comparison with the reference far-field, where it is possible to see a large ripple in the upper lateral lobe as a consequence of the disturbance generated by the reflective surface. After the reflection suppression, the estimated radiation pattern was obtained, which shows a very good agreement with the reference pattern, as observed in Fig. 11(c).

4.2 Noise suppression method

Random noise is one of the errors that limit the accuracy of far-field results, particularly, when measuring a low-sidelobe or a high-performance antenna. One possible source for this error is receiver noise that is present in all measurements. Some comprehensive studies for random noise in near-field measurements have already been presented. For the planar system, two independent analyses with similar results have been proposed in (Newell,1988) and (Hoffman, 1988). A similar study for cylindrical near-field measurements was carried out in (Romeu, 1992). These latter publications derived an expression relating the noise power in the near-field and far-field. The second method proposed in this section is also based on diagnostic techniques and tries to increase the signal-to-noise ratio in the far-field pattern obtained from a planar near-field measurement by reducing the noise power. Increasing the signal-to-noise ratio by reducing the noise power was also proposed in (Koivisto, 2004) and (Foged, 2009). The technique described in these studies can be applied to measurements performed in spherical near-field, and it is based on oversampling to obtain a higher number of spherical modes than required (Jensen, 2004), and thus, to be able to apply a modal filtering. In this second method, a spatial filtering instead of a modal filtering is applied.

In the proposed algorithm, once the planar near-field measurement has been performed, the field at the AUT plane (reconstructed field) is computed. Because the desired contribution is theoretically located inside the dimensions of the AUT, filtering can be applied to cancel the outside contribution due to noise. An analysis to assess the noise behavior and to obtain its statistical parameters was carried out. In the analysis, a complex white Gaussian and space-stationary zero mean noise was considered. From this analysis, it was deduced that, for planar near-field noise with the aforementioned statistical characteristics, the noise in the reconstructed field is a complex, stationary, white Gaussian noise, with zero mean and a variance that is equal to the variance of the noise in the scan plane. Because the noise is kept stationary, i.e., the noise power is identically distributed on the reconstructed surface, and the desired contribution is theoretically concentrated in the region where the AUT is located, a filtering can be applied to cancel the noise out of the AUT dimensions. The definition of filtering appears in (5).

$$F_2(x,y) = \begin{cases} 1 & (x,y) \in \omega_A \\ 0 & (x,y) \in \omega_T - \omega_A \end{cases} \tag{5}$$

where w_T and w_A represent the reconstructed region and the AUT region. Because the noise is identically distributed over the reconstructed surface, the signal-to-noise ratio improvement achieved with the proposed spatial filtering method is the ratio between the surfaces of both reconstructed regions (6).

$$\Delta SNR = \frac{S_{\omega_T}}{S_{\omega_A}} \tag{6}$$

All steps of the proposed algorithm are depicted in Fig. 12. First, the measured data are used to obtain the PWS, referenced to the scan plane, by using an inverse Fourier transform (IFT). The next steps are to reference the PWS to the AUT plane and to calculate the reconstructed field. Then, noise filtering can be used. Finally, a new PWS with less noise power is computed using again an IFT. The validation of this method was carried out by employing the data of the reference measurement presented in the previous method. Gaussian noise with 30 dB less power than the maximum of the acquired data was computationally added. The noise power was chosen to be large so as to ensure a negligible measurement noise. Thus, the far-field obtained from the measured data without additive noise can be used as a reference to compare results before and after noise filtering. The results both for the co-polar and cross-polar pattern are shown in Fig. 13. In this particular case, the improvement calculated as indicated in (6) was equal to 28.27 dB.
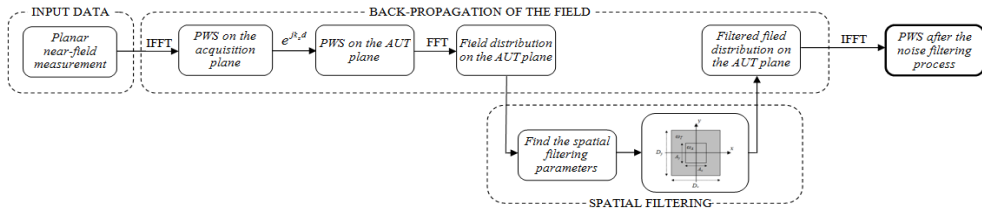

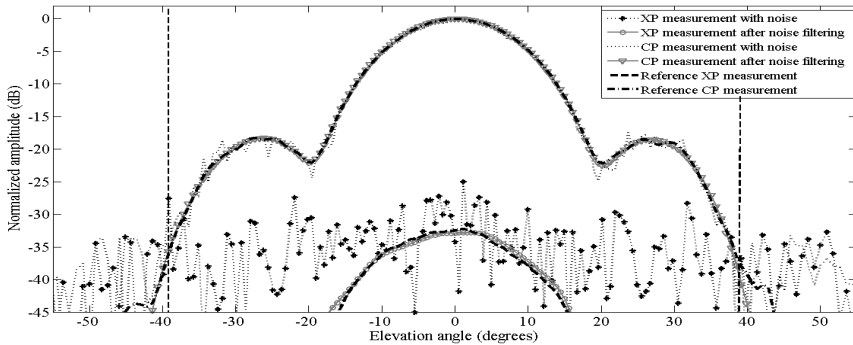Fig. 12. Diagram of the noise suppression method.

Fig. 13. Comparison between the reference pattern, the pattern with noise and the pattern after the noise filtering in $\phi = 90^\circ$ plane. The boundaries of the reliable region are indicated by vertical dotted lines.

4.3 Leakage suppression methods

There are three main sources of leakage signals: the first one is the crosstalk between the reference and the measurement channels in the receiver, although this first source of leakage is normally greatly suppressed by using high quality receivers with a good isolation between channels. The second source is due to connectors, faulty cables or components with poor isolation that act as new emitters distorting the far-field pattern. The last source of leakage is the bias error coming from the receiver's quadrature detector that introduces an

imbalance between the two channels. As a consequence, a complex constant is added to every near-field data sample. Several methods have been proposed to detect and cancel leakage signals. Leakage due to loose connectors, faulty transmission cables or components with poor isolation can be detected by terminating the lines connected to the AUT or the probe and measuring the signal picked up by the receiver (Newell, 1988). Other alternatives try to reduce the undesired effects without any additional measurement by means of analytical compensation techniques (Leatherwood, 2001). The leakage from the receiver bias error cannot be reduced with changes in instrumentation. The first option to suppress the leakage bias error is to perform a complete near-field measurement with both the AUT and the probe terminated and the receiver set to its highest level of averaging (Hindman, 2003). If there is no leakage from cables, the signal measured in this way is directly the bias leakage. Other options without requiring additional measurements are based on estimating that constant by averaging all the measured data that are below a given threshold (Rousseau, 1999) or located outside a certain region (Newell, 1999).

In the present section, two methods to cancel leakage from cables and receiver's quadrature detector in planar near-field measurements are proposed. Both methods are based on a diagnostic technique to determine the field distribution over the AUT plane. In the first case, this information is used to filter out a great leakage contribution. The second method estimates the constant associated to the bias error by averaging the field outside the AUT aperture. If there are undesired sources like loosen connectors, faulty rotary joints or any other component with poor isolation that radiate energy, the measured field can be expressed as a sum of the actual field from the AUT and the field from the leakage (7):

$$E_{meas}(x,y,d) = E_{meas,AUT}(x,y,d) + E_{meas,leakage}(x,y,d) \qquad (7)$$

After back-propagating the field from the scan plane to the AUT plane, the contribution of the leakage is located outside of the AUT dimensions. Therefore, as in the previous examples, a spatial filtering may be applied to cancel the leakage effects. Consequently, the steps of this first leakage suppression method are the same than in the noise suppression method. The validation of this first method is carried out considering the measurement of the previous sections, but including also another pyramidal-horn antenna of lower gain. Moreover an attenuator was placed before this last horn in order to simulate a leakage source, as observed in Fig. 14 (a). By using the acquired data, the reconstructed field was computed. Then, a spatial filtering was applied to cancel the effect of the leakage source. Finally, a new far-field pattern was calculated by means of an inverse Fourier transform of the filtered field, achieving a great improvement, as observed when comparing the results in Fig. 14 (b) and Fig. 14 (c).

The second method presented in this section tries to reduce leakage bias errors without additional measurements. As in the referenced methods, this one is based on an estimation of the constant added to all measured data. Then, the correction is performed by subtracting that estimated constant from the measured data. The main difference of our proposal is the information used to estimate the constant. Before, the measured data are directly employed in the estimation by averaging the near-field samples that satisfy a certain condition in order to not take into account those samples that are dominated by the AUT. In this method, to use the information on the AUT plane, i.e., the estimation is performed after back-propagating the field from the scan plane to the AUT plane is proposed. Then, the samples

located outside of the AUT aperture are employed to calculate the bias constant. Because those samples do not contain any contribution of the AUT, the estimation will be better.

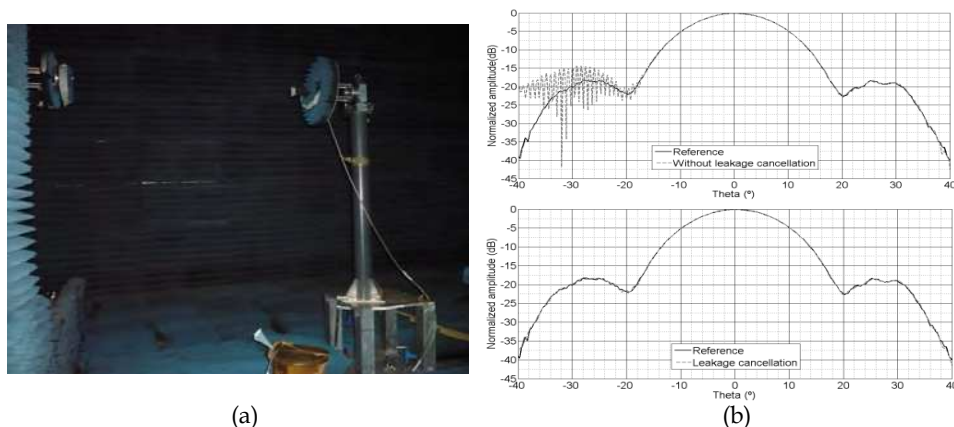|	
(a)	(b)

Fig. 14. (a) Experimental measurement with an additional horn antenna to simulate a leakage source; (b) Comparison between the reference pattern and the pattern with leakage for the φ=90°; (c) Comparison between the reference pattern and the pattern with leakage suppression for the φ =90°.

An example is presented in order to validate this second method. In this case, the reference measurement of the previous section was employed again. Then, a complex constant with 60 dB less amplitude than the maximum of the measured data and phase equal to 45° was computationally added. The estimation of this constant was carried out by using both the method proposed in (Rousseau, 1999) and the alternative proposed here. The results of the estimation are shown in Fig. 15(a) and Fig. 15(b). As observed, a better estimation is obtained by using the method proposed here. Moreover, the range where the constant is

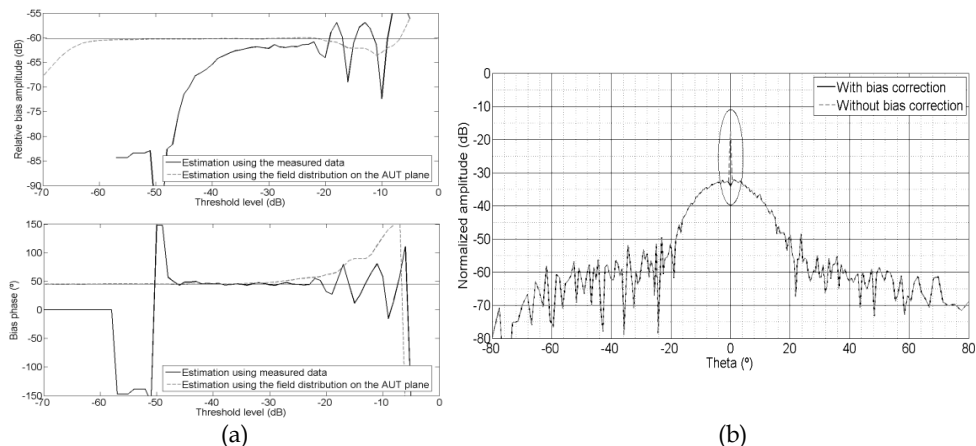|	
(a)	(b)

Fig. 15. (a) Amplitude and (b) phase of the bias error; (c) Comparison between the cross-polar pattern without and with bias correction.

well estimated is much larger. Figure 15(c) demonstrates that after subtracting the estimated constant from the measured data, it is possible to retrieve the reference pattern, removing the peak that appears at the center of k-space.

5. Iterative algorithms to reduce the truncation error in planar, cylindrical and not complete spherical acquisitions

One important requirement to determine exact far-field patterns from near-field acquisitions is the ability to measure the electric or magnetic field that is tangential to an arbitrary surface that encloses the AUT. The planar and cylindrical scanning geometries are mechanically simpler than in the case of the spherical near-field (SNF). Moreover, the spherical near-field to far-field transformation is more complex, requiring more calculations to obtain the far-field pattern from the acquired data. However, the most accurate antenna patterns are obtained using this last type of acquisition because it is the only measurement set-up where the AUT is fully enclosed by the acquisition surface. Therefore, there are no truncation errors in the calculated far-field pattern. In the planar near-field (PNF) and cylindrical near-field (CNF) measurements, because of the finite size of the scan surface, the closed surface condition is never fulfilled, and, consequently, the true far-field pattern is never known in the whole sphere, i.e., the pattern is only valid within the called reliable region. There are some studies that attempt to obtain a good estimation of the true pattern outside of the reliable region. One of these approaches, called the equivalent magnetic current approach (Petre, 1992), presents a method of computing far-fields in the whole forward hemisphere from planar near-field measurements. Another strategy to reduce truncation errors is to rotate the AUT about one or more axes (Gregson, 2005), measuring in different planes and combining them to increase the maximum validity angle. In (Bucci, 2000) and (Bolomey, 2004), the problem of truncation is addressed using a priori information about the AUT. The main idea of this approach is to estimate the near-field data outside of the scanning area by extrapolating the measured data before calculating the far-field pattern. A recent publication (Martini, 2008) also uses a priori information about the AUT in an iterative algorithm to extrapolate the reliable portion of the calculated far-field pattern.

As commented before, truncation errors are always present in PNF and CNF measurements but not in SNF measurements. However, there are special cases, e.g., when measuring electrically large antennas, in which the measurement time may be prohibitively long and an acquisition over the whole sphere is not practical. A solution to reduce the data acquisition time is to measure over a partial sphere. Nevertheless, the new acquisition surface does not fully enclose the AUT, and, as in the PNF and CNF cases, a truncation error appears in the far-field pattern. In (Wittmann, 2002), the truncated spherical near-field data are used to the spherical wave coefficients using forward hemisphere data only, based on a least-squares technique. This method can significantly reduce truncation errors, but it is not efficient for large antennas. This problem is also addressed in (Martini, 2011) where the band-limited property of the spherical wave coefficients is exploited in an iterative algorithm that substitutes the unreliable portion of the measurement sphere with new samples at each iteration. In the present work, a method to reduce truncation errors when measuring the field over truncated surfaces is developed. The method is based on the iterative algorithm that was proposed in (Gerchberg, 1974) and (Papoulis, 1974), and it has already been applied to the PNF case in (Martini, 2008). However, this method can be

applied to any scanning geometry by taking certain considerations into account. Therefore, this work can be viewed as a generalization of that method, although in the proposed method it is not necessary to take samples in surfaces external to the actual scanning area. Therefore the reduction of truncation errors is achieved without increasing the measurement time. A bottleneck of the method presented in (Martini, 2011) may be the time required to find the optimum termination point in the iterative procedure. In this work, a faster procedure based on the Gradient Descent algorithm, with which is possible to obtain the iteration number where the error is minimum, is proposed. Before describing all of the steps of the method, the two orthogonal projection operators that play an important role in the method are presented. The first operator is applied in the spectral domain and defines the reliable portion of the PWS. This first operator is given by

$$A\left(k_x, k_y\right) = \begin{cases} 1 & \forall \left(k_x, k_y\right) \in \Omega_R \\ 0 & \forall \left(k_x, k_y\right) \notin \Omega_R \end{cases} \tag{8}$$

where A is the spectral-truncation operator and Ω_R is the reliable region. The second operator is called band-limited operator and is applied to the field distribution on the AUT plane.

$$h\left(x, y\right) = \begin{cases} 1 & \forall \left(x, y\right) \in \omega_{AUT} \\ 0 & \forall \left(x, y\right) \notin \omega_{AUT} \end{cases} \tag{9}$$

where h stands for the band-limited operator and w_{AUT} is the region where the AUT is located. In the spectral domain, this last operator can be expressed as follows

$$B\, P\left(k_x, k_y\right) = P\left(k_x, k_y\right) * H\left(k_x, k_y\right) \tag{10}$$

being B the band-limited operator defined in the spectral domain, $P(k_x, k_y)$ represents the PWS and H is the inverse Fourier transform of the operator h. The schematic diagram of the method is shown in Fig. 16.
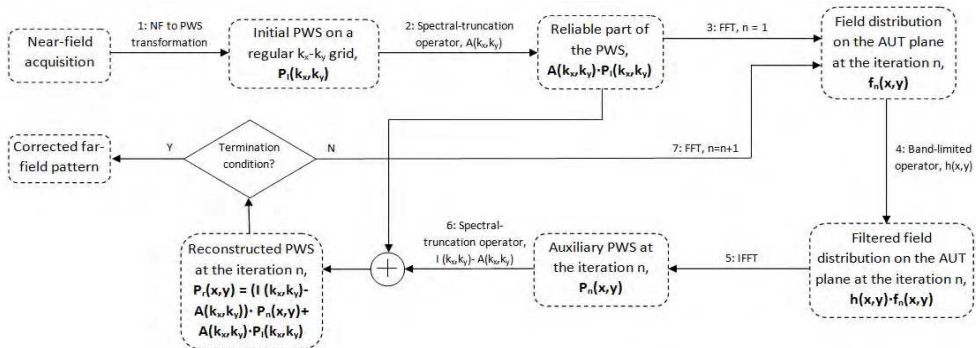

Fig. 16. Diagram of the method to reduce truncation errors.

As mentioned before, the method described in this section can be applied to any scanning geometry. However, the method is only validated here for the CNF case. Other validations for other types of acquisition can be found in (Cano, 2012). For the experiment, a measurement in the CNF range at the UPM was performed. The probe and the AUT consisted of a corrugated conical-horn antenna and a Ku-band reflector with a 40 cm diameter respectively. The data were acquired over a cylinder with a height of 2.7 m and a radius of 2.3 m and with a spatial sampling equal to 0.5λ in the vertical direction and 2.5^{o} in the azimuth. The AUT was also measured in a whole sphere in order to obtain a reference pattern. From inspection of Fig. 17a, it is evident that the truncation error is greatly suppressed, reducing the error outside of the reliable region from 58.2% to 8.9%. A comparison depicted in Fig. 17b shows the reconstructed far-field pattern in the vertical plane versus the truncated and reference far-field pattern.
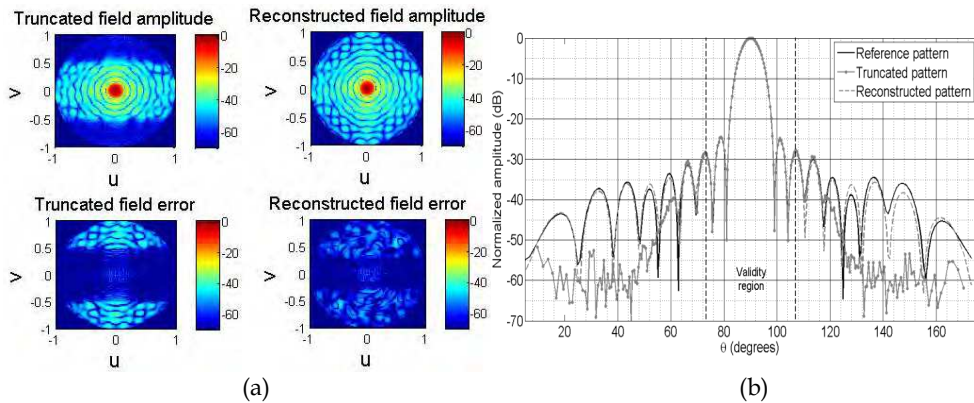

Fig. 17. (a) Far-field pattern and error in dB before and after applying the iterative method; (b) Comparison among the truncated, reconstructed and reference far-field patterns for the reflector in the $\varphi=90^{\text{o}}$ cut.

6. Techniques to improve the quality of the quiet zone in compact ranges

CATR measurement facilities are characterised by a straightforward operation which is able to perform real time antenna measurements along a wide margin of frequencies, whenever reflectors or lenses are used as collimators. In spite of their compactness, CATR facilities operate in far-field conditions. Therefore, the test wave received by the AUT should be a plane wave. The operation of a CATR relies on the planarity of this test wave, inside the "quiet zone" volume. Electromagnetic theory states that the quiet zone region cannot hold a plane wave field distribution, even not with an arbitrarily small volume, for a finite frequency of operation. This is due to the ability of the range's collimator to concentrate the electromagnetic energy within a reduced set of angular directions, following a distribution which is expected to tend to the delta in the angular domain when moving up in frequency. This theoretical constraint must be seen as the first of a set of contributions that affect the quiet zone planarity, and thus, the performance of the CATR which generates it. Usual implementations of the CATR concept focus on minimizing the following quiet zone degradations:

1. Edge diffraction. The collimators are designed so they are able to generate a plane wave inside the quiet zone, while the edge contributions act in the opposite direction. This is minimized in reflector-type collimators through conformal edge treatment: serrated edge and rolled edge geometries (Muñoz-Acevedo, 2012).
2. Collimation scheme. Varied implementations of the field collimation system have been presented, from the classical reflector scheme towards the hologram configuration, going through the dielectric lens. The surface accuracy requirements of a field collimator are increasingly tough when moving up in frequency, being dramatic quiet zone performance reduction the price to pay if they are not fulfilled (Tuovinen, 1992).
3. Reflection from chamber walls. Through the use of RAM, sometimes following conformal wall shapes and different size RAM pyramids depending on their location on the chamber (Bertino, 1998) and (Aubin, 2011).
4. Time gating techniques. They aim to minimize the contribution of reflected signals from spurious field scatterers inside the chamber: test positioners and various unwanted propagation schemes, such as direct ray from the range's feeder or multiple reflections between the range's elements (feeder antenna and field collimators) (Lemanczyk, 2004) and (Boumans, 1987).
5. Feeding scheme. The collimator acts on an incident wave, collimating its phase and amplitude pattern towards the quiet zone. Conventional feeding alternatives impress an amplitude pattern over the collimator, being influenced both by the feeder's pattern and the unequal spherical wave propagation over the incident directions. The main effect on quiet zone is the appearance of an amplitude tapper which can be minimized if several collimators are used in cascade, feeder pattern are made conformal, or both of them (Jones, 1986) and (Kangas, 2003).

Many of these features are used jointly in recent implementations of CATR setups. For a particular facility, its quiet zone distribution can be characterized in diverse ways. The most common are quiet zone probing (Muñoz-Acevedo, 2011) and RCS measurements of canonical objects (Griendt, 1996). These techniques lead to the knowledge of the quiet zone vector field through the amplitude and phase distributions of the components of interest. The described error depends with the frequency at which the CATR is operated. The collimation capabilities of a CATR increase when the frequency is higher. This is due to the fact that both the field collimators and the edge treatment devices are higher, in terms of wavelengths, and their ability to handle the radiation is, thus, superior. However, besides this fact, the required accuracy in terms of surface distortion and range alignment becomes the limiting factor which degrades the potential field collimation performance of the facility down to the actual one. These notes are summarized in Table 2.

This background makes necessary the use of quiet zone information and correction (Viikari, 2007). Solid knowledge of the quiet zone fields implies extensive acquisition campaigns which deal with diverse feed-probe configurations, so the vector field distribution is fully known. This task is very time consuming to be performed , becoming even more critical when increasing the frequency. It is possible however, to acquire the quiet zone distribution in a more time efficient way, without loss of information. The assessment of a particular CATR facility is able to lead to sampling grids which are intrinsically less time consuming and also imply an increase in the acquired field's signal to noise ratio figure, as proposed in (Muñoz-Acevedo, 2011). Fig. 18 summarizes the data acquisition setup and the involved

subsystems. The proposed CATR approach ensures data robustness both in the sense of quiet zone field planarity and distribution stability. The "Field collimation" block follows the notes drawn in (Muñoz-Acevedo, 2012). Accordingly, the direct wave contribution acquired by the probe is isolated from the stray signals through a time gating technique, which the instrumentation "VNA" must be able to perform. The anechoic chamber is properly designed so the measurement environment is isolated from the outer radiation sources. Proper absorber for the frequency range of interest is glued on the inner walls, ceil and floor. These solutions focus on the quiet zone planarity.

Feature	Evolution when increasing frequency
Conformal edge	Increases the scattering performance ($\propto f$).
Collimation scheme	Higher planarity of quiet zone distribution, but stricter surface roughness criteria ($\sigma_{RMS} \propto f^{-1}$).
RAM	Increases the absorbing performance ($\propto f$).
Feeding scheme	Becomes more sensitive to misalignment. ($\propto f$)
Quiet zone acquisitions	Acquisition times for 2D field distributions increase with frequency ($\propto f^2$)

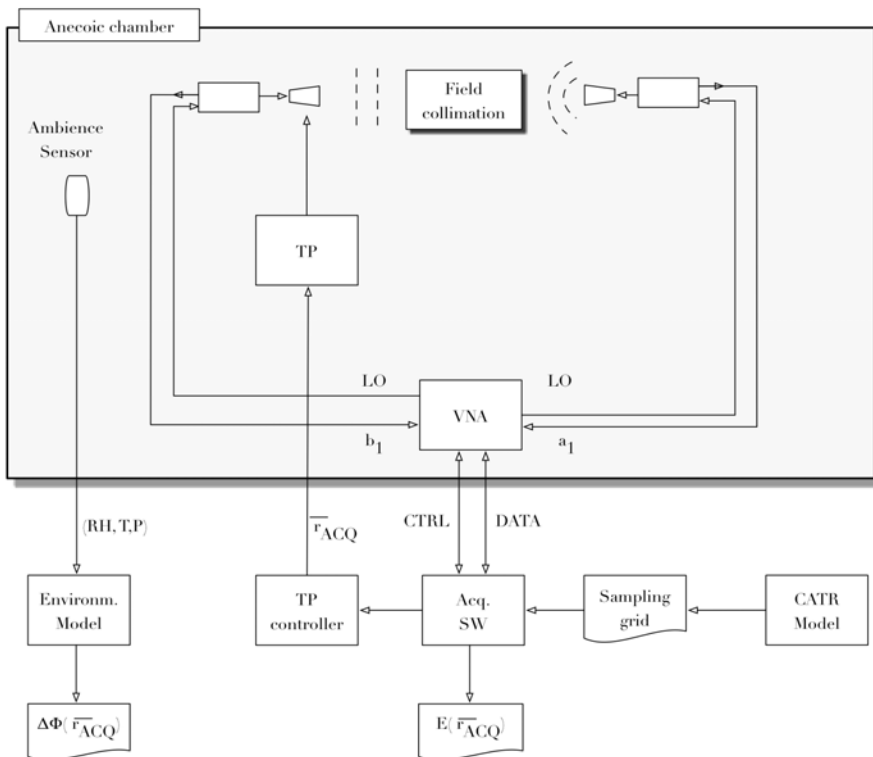Table 2. CATR features vs frequency.

Fig. 18. CATR quiet zone data acquisition setup.

Long term stability of this planarity is achieved through temperature and humidity control inside the chamber and surrounding the instrumentation. The performance of the facility is maximized if these magnitudes are sampled and used as feedback to perform field correction. An ambience sensor samples atmospheric pressure (P), relative humidity (RH) and temperature (T). The environmental model of field propagation uses these magnitudes as inputs and corrects the phase ($\Delta\varphi$) of the probed field taking into account the variation of the air's refractive index $n(T,P,RH)$, as in Eqs. (11, 12). Pressure is measured in *hPa*, T is measured in *K* and Δr states for the path length from the feed towards the test zone, in meters. Coefficients *a, b, c* can be found in the ITU P.453-9 recommendation.

$$\Delta\phi(T,P,RH) = \frac{2\pi}{\lambda_0} \cdot n(T,P,RH) \cdot \Delta r \qquad (11)$$

$$n(T,P,RH) = 1 + \frac{77.6}{T} \cdot \left(P + 4810 \cdot \frac{1}{T} \cdot \frac{RH}{100} \cdot a \cdot \exp\left(\frac{b \cdot (T - T_0)}{(T - T_0) + c} \right) \right) \cdot 10^{-6} \qquad (12)$$

The use of well known probe correction techniques (Bolomey, 2004) is able to subtract the effect of using non-isotropic probes in the field acquisition, while it is unnecessary when the quiet zone is known through RCS techniques instead of probing. The data post-processing scheme which corresponds to the proposed facility of Fig. 18, is shown in Fig. 19.
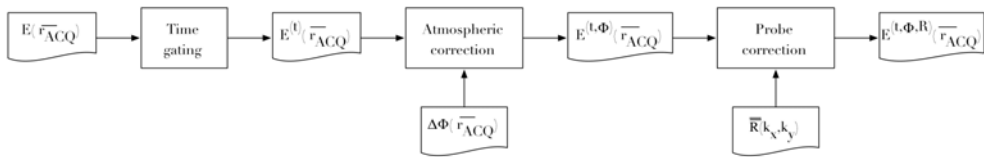

Fig. 19. CATR quiet data post-processing scheme.

7. Conclusions

This chapter has presented different correction techniques to be applied in antenna measurements. In particular, the authors have analyzed the extension of the pattern averaging technique to improve the accuracy of the measurements by minimizing the room scattering or mechanical errors. In the next section, a source reconstruction technique has been used to reduce the measurement errors associated to noise, leakage or scattering. In section 6, the iterative procedure called Gerchberg-Papoulis, applied previously for planar acquisitions, has been extended to cylindrical and partial sphere near field antenna measurements. Finally, section 7 has shown an algorithm to correct some of the classical errors that affect the compact antenna test ranges. In particular, the authors have presented an algorithm to compensate the errors associated to variations in temperature and humidity, important for submillimeter wave frequencies. Therefore, this chapter explains a synthesis of old and new methods for improving the quality of the classical antenna measurement systems, using post-processing tools.

8. Acknowledgments

9. References

A. Alexandridis (NCSRD), et al. (December 2007), "Recommendations and Comparative Investigation for Near-Field Antenna Measurement Techniques and Procedures", Deliverable A1.2D2, "Standardization of Antenna Measurement Techniques", Contract FP6-IST 026957, Antenna Centre of Excellence (ACE).

A. C. Newell (June 1988), "Error Analysis Techniques for Planar Near-Field Measurements", IEEE Transactions on Antennas and Propagation, Vol. 36, No. 6, pp. 754-768, June 1988.

A. C. Newell amd C. F. Stubenrauch (June 1988), "Effect of Random Errors in Planar Near-Field Measurement", IEEE Transactions on Antennas and Propagation, Vol. 36, No. 6, pp. 769-773.

A. C. Newell and A. D. Yaghjian (June 1975), "Study of Errors in Planar Near-Field Measurements", Antennas and Propagation Society International Symposium 1975, pp. 470-473.

A. D. Yaghjian (January, 1986), "An overview of near-field antenna measurements," IEEE Trans. Antennas Propagat., vol. AP-34, No. 1, pp. 30-44.

A. Muñoz-Acevedo, L. Rolo, M. Paquay, M. Sierra-Castañer (2011), "Accurate and Time Efficient Quiet Zone Acquisition Technique for the Assessment of ESA's CATR at Millimeter Wavelengths", XXXIII AMTA Symposium, Denver, Colorado.

A. Muñoz-Acevedo, M. Sierra-Castañer (2012) "An Efficient Hybrid GO-PWS Algorithm to Analyze Conformal Serrated- Edge Reflectors for Millimeter-Wave Compact Range", IEEE Transactions on Antennas and Propagation (accepted).

A. Newell (1999), "Methods to estimate and reduce leakage bias errors in planar near-field antenna measurements," presented at Antenna Measurement Techniques Assosiation 1999, Monterey, California, USA.

A. Newell, G. Hindman (November 2008), "Mathematical Absorber Suppression (MARS) for Anechoic Chamber Evaluation & Improvement", Proceedings of the AMTA Symposium, Boston, USA.

A. Papoulis (September 1975), "A new algorithm in spectral analysis and bandlimited extrapolation," IEEE Trans. Circuits Syst., vol. CAS-22, no. 9, pp- 735-742.

B. N. Taylor and C. E. Kuyatt (1994), "Guidelines for Evaluating and Expressing the Uncertainty of NIST Measurement Results", National Institute of Standards and Technology (NIST) Technical Note 1297, 1994 Edition, United States Department of Commerce Technology Administration.

C. Cappellin (September 2007), "Antenna diagnostics for spherical near-field antenna measurements," Ph.D. dissertation, Dept. Elect. Eng., Danmarks Tekniske Universitet, Copenhague, Denmark.

C. Cappellin, A. Frandsen, and O. Breinbjerg (October 2008), "Application of the SWE-to-PWE antenna diagnostics technique to an offset reflector antenna," IEEE Antennas Propagat. Mag., vol. 50, No. 5, pp. 204-213.

D. A. Leatherwood and E. B. Joy (December 2001), "Plane wave, pattern subtraction, range compensation," IEEE Trans. Antennas Propagat., vol. 49, no. 12, pp. 1843-1851.

D. A. Leatherwood, E. B. Joy (December 2001), "Plane wave, pattern subtraction, range compensation," IEEE Trans. Antennas Propagat., vol. 49, No. 12, pp. 1843-1851.

D. G. Gentle, A. Beardmore, J. Achkar, J. Park, K. MacReynolds, J. P. M. De Vreede, (September 2003), "National Physical Laboratory (NPL) Report CETM 46: Measurement Techniques and Results of an Intercomparison of Horn Antenna Gain in IEC-R 320 at Frequencies of 26.5, 33.0 and 40.0 GHz".

D. N. Black and E. B. Joy (April 1995), "Test zone field compensation," IEEE Trans. Antennas Propagat., vol. 43, No. 4, pp. 362-368.

D. W. Hess (October 2002), "An Expanded Approach to Spherical Near-Field Uncertainty Analysis", AMTA 24th Annual Meeting and Symposium, Cleveland, OH.

D. Young, D. E. Svoboda, and W. D. Burnside (July 1973), "A comparison of time- and frequency-domain measurement techniques in antenna theory," IEEE Trans. Antennas Propagat., vol. 21, No. 4, pp. 581-583.

E. Martini, O. Breinbjerg, and S. Maci (November 2008), "Reduction of truncation errors in planar near-field aperture antenna measurements using the Gerchberg-Papoulis algorithm," IEEE Trans. Antennas Propagat., vol. 56, no. 11, pp. 3485-3493.

E. Martini, S. Maci, and L. J. Foged (April 2011), "Spherical near field measurements with truncated scan area," in Proc. European Conf. Antennas Propag. 2011, Rome, pp. 3412-3414.

E. N. Clouston, P. A. Langsford, and S. Evans (April, 1988), "Measurement of anechoic chamber reflections by time-domain techniques," IEE Proc. H, Microwaves Antennas Propagt., vol. 135, Pt. H, No. 2, pp. 93-97.

F. J. Cano-Fácila, S. Burgos, and M. Sierra-Castañer (April 2011), "Novel method to improve the signal-to-noise ratio in the far-field results obtained from planar near-field measurements," IEEE Antennas Propagat. Magazine.

F. J. Cano-Fácila, S. Burgos, F. Martín, and M. Sierra-Castañer (March 2011), "New reflection suppression method in antenna measurement systems based on diagnostic techniques," IEEE Trans. Antennas Propagat., vol. 59, No. 3, pp. 941-949.

F. J. Cano-Fácila, S. Pivnenko, and M. Sierra-Castañer (2012), "Reduction of truncation errors in planar, cylindrical and partial spherical near-field antenna measurements," to be published in Int. J Antennas Propagat.

F. Jensen and A. Frandsen (October 2004), "On the number of modes in spherical wave expansion," in Proc. 2004 Antenna Meaurement. Techniques Assoc., AMTA, Stone Mountain Park, GA, pp. 489-494.

G. A. Burrell and A. R. Jamieson (September 1973), "Antenna radiation pattern measurement using time-to-frequency transformation (TFT) techniques," IEEE Trans. Antennas Propagat., vol. 21, No. 5, pp. 702-704.

G. Hindman, A. C. Newell (February 2007), "Simplified Spherical Near-Field Accuracy Assessment", IEEE Antennas and Propagation Magazine, Vol. 49, No. 1.

G. Hindman, A. Newell, and P. N. Betjes (September 2003), "Error correction techniques for near-field antenna measurements," presented at the International ITG Conference on Antennas 2003, INICA 2003, Berlin, Germany.

I. Bertino, U. Bozzetti, G. Ariano (1998) "A State of the Art Anechoic Chamber for Air vehicle Testing at Alenia Aeronautica", XX AMTA Symposium, Montreal, Canada.

International Organization for Standardization ISO/IEC 98 Publications (1995), "Guide to the Expression of Uncertainty in Measurement (GUM)", International Organization for Standardization, Geneva, Switzerland, 1995, ISBN: 92-67-10188-9.

J. Appel-Hansen (July 1973), "Reflectivity level of radio anechoic chambers," IEEE Trans. Antennas Propagt., vol. AP21, No. 4, pp. 490-498.

J. Aubin, M. Winebrand, V. Vinogradov (July, 2011) "Experimental validation of the "Two - Level GTD" method for design of anechoic chambers," 2011 IEEE International Symposium on Antennas and Propagation, pp.1893-1896.

J. B. Hoffman and K. R. Grimm (June 1988), "Far-Field Uncertainty Due to Random Near-Field Measurement Error", IEEE Transactions on Antennas and Propagation, Vol. 36, No. 6, pp. 774-780.

J. C. Bolomey, et al (February 2004), "Reduction of truncation error in near-field measurement of antennas of base-station mobile communication systems," IEEE Trans. Antennas Propag., vol. AP-52, no. 2, pp. 593–602.

J. E. Hansen (1997), "Definition, design, manufacture, test and use of a 12 GHz Validation Standard Antenna", Executive Summary, ESTEC contract No. 7407/87/NL /PB, Technical Report R672, Tech. Univ. of Denmark.

J. E. Hansen (ed.) (1988), "Spherical Near-Field Antenna Measurements", Peter Peregrinus Ltd., on behalf of IEE, London, UK.

J. J. H. Wang (June 1988), "An examination of the theory and practices of planar near-field measurement," IEEE Trans. Antennas Propagat., vol. 36, No. 6, pp. 746-753.

J. Jones, (1986) "Prime Focus Feeds for the Compact Range", VIII AMTA Symposium, Ottawa, Canada.

J. Lemanczyk, J. Hartmann, D. Fasold (2004) "Evaluation of hard gating in the ESA/ESTEC CPTR", XXVI AMTA Symposium 2004, Atlanta, Georgia.

J. Romeu, L. Jofre and A. Cardama (January 1992), "Far-Field Errors Due to Random Noise in Cylindrical Near-Field Measurements", IEEE Transactions on Antennas and Propagation, Vol. 40, No. 1, pp. 79-84.

J. Tuovinen, A. Vasara, A. Räisänen (1992), "A hologram type of Compact Antenna Test Range", XIV AMTA Symposium, Columbus, Ohio.

L. A. Muth (May 1988), "Displacement Errors in Antenna Near-Field Measurements and Their Effect on the Far-Field", IEEE Transactions on Antennas and Propagation, Vol. 36, No. 5, pp. 581-591.

L. J. Foged and M. Faliero (November 2009), "Random noise in spherical near-field systems," in Proc. 2009 Antenna Meaurement. Techniques Assoc., AMTA, Salt Lake City, UT, pp. 135-138.

M. Boumans, S. Brumley (1987) "Hardware Gating Improves HP 8510 based RCS Measurement Systems", IX AMTA Symposium, Seattle, Washington.

M. Nagatoshi, M. Hirose, H. Tanaka, S. Kurokawa, and H. Morishita (July 2008), "A method of pattern measurement to cancel reflection waves in anechoic chamber," in Antennas Propagt. Soc. Int. Symp. 2008, San Diego, CA, pp. 1-4.

M.A.J. Griendt, V.J. Vokurka, J. Reddy, J. Lemanczyk (1996)"Evaluation of a CPTR using an RCS Flat Plate Method", XVIII AMTA Symposium, Seattle, Washington.

O. M. Bucci, G. D'Elia, and M. D. Migliore (2000), "A new strategy to reduce the truncation error in near-field far-field transformation," Radio Sci., vol. 35, no. 1, pp. 3–17.

P. Koivisto (2004), "Reduction of errors in antenna radiation patterns using optimally truncated spherical wave expansion," Progress In Electromagnetic Research, vol. pier-47, pp. 313-333.

P. Petre and T. K. Sarkar (November 1992), "Planar near-field to far-field transformation using an equivalent magnetic current approach," IEEE Trans. Antennas Propagat., vol. 40, No. 11, pp. 1348-1356.

P. R. Rousseau (1999), "An algorithm to reduce bias errors in planar near-field measurement data," presented at Antenna Measurement Techniques Assosiation 1999, Monterey, California, USA.

R. C. Johnson, H. A. Ecker, and J. S. Hollis (December 1973), "Determination of far-field antenna patterns from near-field measurements," Proc. IEEE, vol. 61, No. 12, pp. 1668-1694.

R. C. Wittmann, C. F. Stubenrauch, and M. H. Francis (2002), "Spherical scanning measurements using truncated data sets," in AMTA Proc. 2002, Cleveland, OH, pp. 279-283.

R. J. Lytle (November 1972), "Ground reflection effects upon radiated and received signals as viewed via image theory," IEEE Trans. Antennas Propagat., vol. AP-20, No. 6, pp. 736-741.

R. W. Gerchberg (May 1974), "Super-resolution through error energy reduction," Opti. Acta, vol. 21, no. 9, pp. 709-720, May 1974.

S. Burgos (September 2009), "Contribution to the uncertainty evaluation in the measurement of the main antenna parameters", , Doctoral Thesis, Technical University of Madrid (UPM), Madrid, Spain.

S. Burgos, M. Sierra Castañer, F. Martín, F. Cano, J. L. Besada, (April 2010), "Error analysis and simulator in cylindrical near-field antenna measurement systems", book entitled "Advances in Measurements Systems", Pages: 289 – 314, Edited by Milind Kr Sharma, ISBN: 978-953-7619-X-X, Vienna, Austria.

S. F. Gregson, C. G. Parini, and J. McCormick (December 2005), "Development of wide-angle pattern measurements using a probe-corrected polyplanar near-field measurement technique," IEE Proc. Microw. Antennas Propag., vol. 152, pp. 563-572, no. 6.

S. Loredo, M. R. Pino, F. Las-Heras, and T. K. Sarkar (February 2004), "Echo identification and cancellation techniques for antenna measurement in non-anechoic test sites," IEEE Antennas Propagat. Mag., vol. 46, No. 1, pp. 100-107.

S. Pivnenko, J. M. Nielsen, O. Breinbjerg (May 2006), "Electrical Uncertainties In Spherical Near-Field Antenna Measurements", Proceedings of the First Antenna

Measurements Techniques Association Europe (AMTA Europe) Symposium, pp.183-186, Munich.

V. Kangas, J. Lemanczyk (2003), "Compact Range Defocused Quiet Zone Characterization", XXV AMTA Symposium, Irvine, California.

V. Viikari (April 2007), "Antenna Pattern Correction Techniques at Submillimeter Wavelengths". Helsinki University of Technology. Dissertation for the degree of Doctor of Science in Technology.

Y. Álvarez, F. Las-Heras, and M. R. Pino (December 2007), "Reconstruction of equivalent currents distribution over arbitrary three-dimensional surfaces based on integral equation algorithms," IEEE Trans. Antennas Propagat., vol. 55, No. 12, pp. 3460-3468.
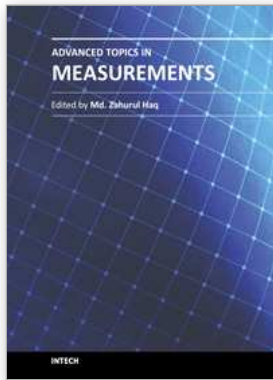
Advanced Topics in Measurements

Edited by Prof. Zahurul Haq

ISBN 978-953-51-0128-4

Hard cover, 400 pages

Publisher InTech

Published online 07, March, 2012

Published in print edition March, 2012

Measurement is a multidisciplinary experimental science. Measurement systems synergistically blend science, engineering and statistical methods to provide fundamental data for research, design and development, control of processes and operations, and facilitate safe and economic performance of systems. In recent years, measuring techniques have expanded rapidly and gained maturity, through extensive research activities and hardware advancements. With individual chapters authored by eminent professionals in their respective topics, Advanced Topics in Measurements attempts to provide a comprehensive presentation and in-depth guidance on some of the key applied and advanced topics in measurements for scientists, engineers and educators.

How to reference

In order to correctly reference this scholarly work, feel free to copy and paste the following:

Manuel Sierra-Castañer, Alfonso Muñoz-Acevedo, Francisco Cano-Fácila and Sara Burgos (2012). Overview of Novel Post-Processing Techniques to Reduce Uncertainty in Antenna Measurements, Advanced Topics in Measurements, Prof. Zahurul Haq (Ed.), ISBN: 978-953-51-0128-4, InTech, Available from: http://www.intechopen.com/books/advanced-topics-in-measurements/overview-of-novel-post-processing-techniques-to-reduce-uncertainty-in-antenna-measurements

INTECH

open science | open minds